Chebyshev collocation Dirichlet-to-Neumann map method for diffraction gratings

Dawei Song[1,2,3] and Ya Yan Lu[3]

[1] *Joint Advanced Research Center of University of Science and Technology of China and City University of Hong Kong, Suzhou, Jiangsu, China*

[2] *Department of Mathematics, University of Science and Technology of China Hefei, Anhui, China*

[3] *Department of Mathematics, City University of Hong Kong, Kowloon, Hong Kong*

For diffraction gratings with layered refractive index profiles, the Fourier modal method is widely used. However, it is quite expensive to calculate the eigenmodes for each layer, especially when the structure involves absorptive media. In this paper, we develop an efficient method that avoids the eigenvalue problems based on the so-called Dirichlet-to-Neumann (DtN) map. For each layer, the DtN map is an operator that maps the wave field to its normal derivative on one period of the boundaries of the layer, and it is approximated by a matrix. An efficient procedure for computing the DtN map is developed based on a Chebyshev collocation method and a fourth order finite difference method for discretizing the uniform and the periodic directions, respectively. The efficiency and accuracy of our method are illustrated by numerical examples.

OCIS codes: 050.1950, 000.4430

1. Introduction

Numerical methods are essential tools in the design and optimization of diffraction gratings [1, 2]. In principle, when the problem is formulated on one period of the structure, it can be solved by standard numerical methods, such as the finite element method [3]. However, these general methods give rise to large, complex, indefinite linear systems that are relatively expensive to solve. Less general methods that take advantage of available geometric features are often more efficient. Special numerical methods for diffraction gratings include the exact modal method [4–6], the Fourier modal method (FMM) [7–10], the finite difference modal method [12], the differential method [2, 13, 14], the boundary integral equation method [15–

18], etc. All modal methods require that the structure consists of uniform layers, so that the wave field can be expanded in eigenmodes in each layer. FMM calculates the eigenmodes based on Fourier series expansions. Since it is relatively easy to implement, FMM is extremely popular. Notice that computing the eigenmodes in each layer is usually the most expensive part of FMM.

In this paper, we develop a new method for diffraction gratings with uniform layers. Instead of computing the eigenmodes in each layer, we calculate an operator that maps the wave field to its normal derivative at the boundaries of the layer. In practice, this operator, the so-called Dirichlet-to-Neumann (DtN) map, is approximated by a matrix, and it can be efficiently calculated using a highly accurate Chebyshev collocation method and a fourth order finite difference method to discretize the uniform and periodic directions, respectively. In previous work [19–23], the DtN formalism has been used to analyze periodic arrays of cylinders and piecewise uniform waveguides. For circular cylinders, the DtN maps are constructed from cylindrical harmonics [19]. For uniform waveguide segments, the Chebyshev collocation method was used with a second order finite difference method in the transverse direction to approximate the DtN maps [20]. In the present work, the fourth order finite difference scheme first developed in [24] is used to discretize the periodic direction. As illustrated in numerical examples, our new method is more accurate than FMM, when the same degrees of freedom are used in the discretization, and it is also more efficient than FMM, since the time consuming eigenvalue decomposition is avoided and the DtN map can be calculated efficiently.

2. Problem formulation

We consider layered diffraction gratings which are two-dimensional (2D) structures with a one-dimensional (1D) periodicity. Let $\{x, y, z\}$ be a Cartesian coordinate system, we assume that the structure is invariant in the z direction, and it is specified by a z-independent dielectric function $\varepsilon = \varepsilon(\mathbf{r})$ where $\mathbf{r} = (x, y)$. The actual grating is in the region given by $0 < y < D$ where D is a positive constant, and it is sandwiched between two homogeneous media. We have

$$\varepsilon(\mathbf{r}) = \begin{cases} \varepsilon_t, & y > D, \\ \varepsilon_b, & y < 0, \end{cases} \tag{1}$$

where ε_t and ε_b are constants. Meanwhile, the grating is periodic in the x direction with period L, therefore

$$\varepsilon(x + L, y) = \varepsilon(x, y). \tag{2}$$

We also assume that the grating is a layered structure consisting of y-invariant layers. More precisely, we have $0 = y_0 < y_1 < ... < y_m = D$, such that the dielectric function in the j-th

layer (y_{j-1}, y_j) is y-independent:

$$\varepsilon(\mathbf{r}) = \varepsilon_j(x), \quad y_{j-1} < y < y_j, \tag{3}$$

where ε_j is a function of x only. In Fig. 1, we show a grating with three y-invariant layers in

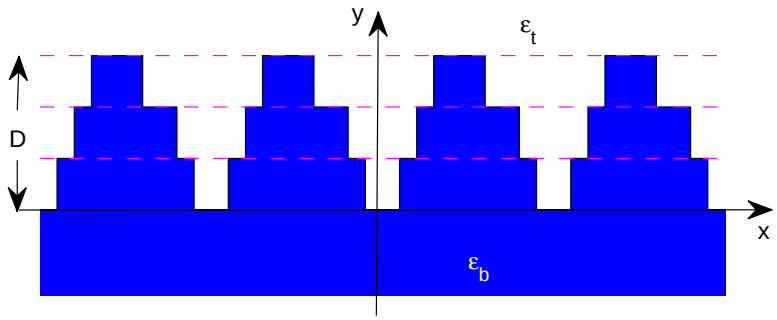

Fig. 1. A grating with three uniform layers in the grating region.

the grating region.

For these 2D structures, if the wave field is also invariant in z, we can separately consider two polarizations. Assuming that the time dependence is $\exp(-i\omega t)$, where ω is the angular frequency, the frequency domain Maxwell's equations are reduced to

$$\rho\frac{\partial}{\partial x}\left(\frac{1}{\rho}\frac{\partial u}{\partial x}\right) + \rho\frac{\partial}{\partial y}\left(\frac{1}{\rho}\frac{\partial u}{\partial y}\right) + k_0^2\varepsilon\, u = 0, \tag{4}$$

where $k_0 = \omega/c$ is the free space wavenumber and c is the speed of light in vacuum. For the E polarization, u is the z component of the electric field and $\rho = 1$; for the H polarization, u is the z component of the magnetic field and $\rho = \varepsilon$. In the top region, $y > D$, we specify a plane incident wave

$$u^{(i)}(\mathbf{r}) = \exp[i(\alpha_0 x - \beta_0^{(t)} y)], \quad y > D, \tag{5}$$

where $\beta_0^{(t)}$ is positive and it satisfies $\alpha_0^2 + [\beta_0^{(t)}]^2 = k_0^2\varepsilon_t$. If θ_0 is the angle between the wave vector $(\alpha_0, -\beta_0^{(t)})$ and the y axis, then

$$\alpha_0 = k_0\sqrt{\varepsilon_t}\sin\theta_0, \quad \beta_0^{(t)} = k_0\sqrt{\varepsilon_t}\cos\theta_0. \tag{6}$$

The incident wave gives rise to a reflected wave $u^{(r)}$ and a transmitted wave $u^{(t)}$ in the top $(y > D)$ and the bottom $(y < 0)$ regions, respectively. We have

$$u(\mathbf{r}) = \begin{cases} u^{(i)}(\mathbf{r}) + u^{(r)}(\mathbf{r}), & y > D, \\ u^{(t)}(\mathbf{r}), & y < 0. \end{cases}$$

It is well known that the reflected and transmitted waves can be expanded as

$$u^{(r)}(\mathbf{r}) = \sum_{j=-\infty}^{\infty} R_j \exp[i(\alpha_j x + \beta_j^{(t)} y)], \quad y > D, \tag{7}$$

$$u^{(t)}(\mathbf{r}) = \sum_{j=-\infty}^{\infty} T_j \exp[i(\alpha_j x - \beta_j^{(b)} y)], \quad y < 0, \tag{8}$$

where T_j and R_j are the transmission and reflection coefficients, and

$$\alpha_j = \alpha_0 + \frac{2j\pi}{L}, \quad \beta_j^{(t)} = \sqrt{k_0^2 \varepsilon_t - \alpha_j^2}, \quad \beta_j^{(b)} = \sqrt{k_0^2 \varepsilon_b - \alpha_j^2}. \tag{9}$$

Mathematically, the problem can be formulated on the rectangular domain S given by $S = \{(x, y) \mid 0 < x < L,\ 0 < y < D\}$. Due to the periodicity of the structure and the x-dependence of $u^{(i)}$, the wave field satisfies the quasi-periodic condition $u(x+L, y) = \gamma u(x, y)$, where $\gamma = \exp(i\alpha_0 L)$. This leads to

$$u|_{x=L} = \gamma u|_{x=0}, \quad \left.\frac{1}{\rho}\frac{\partial u}{\partial x}\right|_{x=L^+} = \gamma \left.\frac{1}{\rho}\frac{\partial u}{\partial x}\right|_{x=0^+}. \tag{10}$$

At $y = 0$ and $y = D$, we can write down exact boundary conditions as

$$\frac{\partial u}{\partial y} = \mathcal{S}_b\, u, \qquad y = 0^-, \tag{11}$$

$$\frac{\partial u}{\partial y} = \mathcal{S}_t\, u - 2\mathcal{S}_t\, u^{(i)}, \quad y = D^+, \tag{12}$$

where $\mathcal{S}_b$ and $\mathcal{S}_t$ are linear operators satisfying

$$\mathcal{S}_b \exp(i\alpha_j x) = -i\beta_j^{(b)} \exp(i\alpha_j x), \tag{13}$$

$$\mathcal{S}_t \exp(i\alpha_j x) = i\beta_j^{(t)} \exp(i\alpha_j x), \tag{14}$$

for all integer j [19, 25]. In practice, if one period of x is discretized by N points, the operators $\mathcal{S}_b$ and $\mathcal{S}_t$ are approximated by $N \times N$ matrices. More precisely, we first truncate integer j to $-N/2 \le j < N/2$ if N is even and to $|j| \le (N-1)/2$ if N is odd, then find matrices (approximating $\mathcal{S}_b$ and $\mathcal{S}_t$) whose eigenvalues are $-i\beta_j^{(b)}$ and $i\beta_j^{(t)}$, and the corresponding eigenvectors are $\exp(i\alpha_j x)$ evaluated at the N points of x. In conclusion, we obtain a boundary value problem consisting of Eq. (4) and boundary conditions (10)-(12).

3. Dirichlet-to-Neumann map method

For layered diffraction gratings where each layer is y-invariant, we first calculate the Dirichlet-to-Neumann (DtN) map for each layer, then use these operators to find the solution. For the j-th layer given by $y_{j-1} < y < y_j$, the DtN map is a 2×2 matrix operator $\mathcal{M}^{(j)}$ satisfying

$$\mathcal{M}^{(j)} \begin{bmatrix} u_{j-1} \\ u_j \end{bmatrix} = \begin{bmatrix} \mathcal{M}_{11}^{(j)} & \mathcal{M}_{12}^{(j)} \\ \mathcal{M}_{21}^{(j)} & \mathcal{M}_{22}^{(j)} \end{bmatrix} \begin{bmatrix} u_{j-1} \\ u_j \end{bmatrix} = \begin{bmatrix} \partial_y u_{j-1}^+ \\ \partial_y u_j^- \end{bmatrix}, \tag{15}$$

where u is an arbitrary solution of the Helmholtz equation (4) and the quasi-periodic condition (10), $u_{j-1} = u(x, y_{j-1})$, $u_j = u(x, y_j)$, $\partial_y u_{j-1}^+$ and $\partial_y u_j^-$ denote $\partial_y u$ at y_{j-1}^- and y_j^+, respectively. For the H polarization, $\partial_y u$ is not always continuous, therefore we use its interior limit in the above definition. The matrix operator $\mathcal{M}^{(j)}$ is given in 2×2 form where each entry is an operator. If x is discretized by N points, then $\mathcal{M}^{(j)}$ is approximated by a $(2N) \times (2N)$ matrix, and the entries $\mathcal{M}_{kl}^{(j)}$, for $1 \le k, l \le 2$, are approximated by $N \times N$ matrices. Since the layer is y-invariant, it has a reflection symmetry which implies that $\mathcal{M}_{12}^{(j)} = -\mathcal{M}_{21}^{(j)}$ and $\mathcal{M}_{22}^{(j)} = -\mathcal{M}_{11}^{(j)}$. Therefore, we only need to calculate two blocks $\mathcal{M}_{11}^{(j)}$ and $\mathcal{M}_{12}^{(j)}$. In Section 4, we present an efficient method for computing $\mathcal{M}^{(j)}$.

Once the DtN maps are calculated, we can set up a linear system of equations for u_0, u_1, ..., u_m, based on the continuity of $\rho^{-1}\partial_y u$. We have

$$\frac{1}{\rho_0^-}\mathcal{S}_b\, u_0 = \frac{1}{\rho_0^+}\left[\mathcal{M}_{11}^{(1)}\, u_0 + \mathcal{M}_{12}^{(1)}\, u_1\right], \tag{16}$$

$$\frac{1}{\rho_j^-}\left[\mathcal{M}_{21}^{(j)}\, u_{j-1} + \mathcal{M}_{22}^{(j)}\, u_j\right] = \frac{1}{\rho_j^+}\left[\mathcal{M}_{11}^{(j+1)}\, u_j + \mathcal{M}_{12}^{(j+1)}\, u_{j+1}\right], \quad 1 \le j < m, \tag{17}$$

$$\frac{1}{\rho_m^-}\left[\mathcal{M}_{21}^{(m)}\, u_{m-1} + \mathcal{M}_{22}^{(m)}\, u_m\right] = \frac{1}{\rho_m^+}\left[\mathcal{S}_t\, u_m - 2\mathcal{S}_t\, u_m^{(i)}\right], \tag{18}$$

where $u_m^{(i)}$ is the incident wave evaluated at $y_m = D$, and $\rho_j^\pm$ denotes ρ at $y_j^\pm$. Notice that the boundary conditions at $y = 0$ and $y = D$ have been used to derive equations (16) and (18). For a lamellar grating with only one y-invariant layer in the grating region ($m = 1$), only the first and last equations remain. If one period of x is discretized by N points, then u_j is a vector of length N, the linear system (16), (17) and (18) involves $(m+1)N$ unknowns, and its coefficient matrix has a block tridiagonal form with $N \times N$ blocks. The standard Gaussian elimination for banded matrices can be used, and it requires $O(mN^3)$ operations.

As an alternative to solving the linear system above, we can use the operator marching scheme developed in [19]. To take care of the possible material discontinuities (for the H polarization), we introduce operators $\mathcal{Q}_j^-$, $\mathcal{Q}_j^+$ and $\mathcal{Y}_j$ satisfying

$$\mathcal{Q}_j^-\, u_j = \partial_y u_j^-, \quad \mathcal{Q}_j^+\, u_j = \partial_y u_j^+, \quad \mathcal{Y}_j\, u_j = u_0, \tag{19}$$

where u is any solution of (4), (10) and (11), u_j and $\partial_y u_j^\pm$ are defined as before. In the discrete case, these operators are represented by $N \times N$ matrices. At $y = 0$, using the boundary condition (11) and the definition of $\mathcal{Y}_0$, we obtain:

$$\mathcal{Q}_0^- = \mathcal{S}_b, \quad \mathcal{Y}_0 = I, \tag{20}$$

where I is the identity operator. The continuity of $\rho^{-1}\partial_y u$ gives

$$\frac{1}{\rho_j^+}\mathcal{Q}_j^+ = \frac{1}{\rho_j^-}\mathcal{Q}_j^-, \quad j = 0, 1, ..., m. \tag{21}$$

For the j-th layer, we can march the two operators from y_{j-1}^+ to y_j^- by

$$\mathcal{Z} = \left[\mathcal{Q}_{j-1}^+ - \mathcal{M}_{11}^{(j)}\right]^{-1} \mathcal{M}_{12}^{(j)}, \tag{22}$$

$$\mathcal{Q}_j^- = \mathcal{M}_{22}^{(j)} + \mathcal{M}_{21}^{(j)} \mathcal{Z}, \tag{23}$$

$$\mathcal{Y}_j = \mathcal{Y}_{j-1} \mathcal{Z}. \tag{24}$$

The above formulae can be derived from the definition of $\mathcal{M}^{(j)}$. More details are given in [19]. Based on equations (20)-(24), we can find $\mathcal{Q}_m^+$ and $\mathcal{Y}_m$ following a simple recursive process. After that, we can calculate u_m and u_0 from

$$[\mathcal{Q}_m^+ - \mathcal{S}_t] u_m = -2\mathcal{S}_t\, u_m^{(i)}, \tag{25}$$

$$u_0 = \mathcal{Y}_m\, u_m, \tag{26}$$

where Eq. (25) is the boundary condition (12). The reflected wave can calculated by subtracting the incident wave from u_m. Although the operator marching scheme also requires $O(mN^3)$ operations, its memory requirement is only $O(N^2)$ and it is independent of m.

4. Chebyshev collocation method

From the previous section, it is clear that our method is competitive only if we can efficiently calculate the DtN map for each y-invariant layer. In this and the following sections, we show that the DtN map of a layer can be calculated using $O(qN^2)$ operations, where N is the number of points for discretizing one period of x and q is much smaller than N. In comparison, the Fourier or finite difference modal method requires $O(N^3)$ operations to compute the eigenvalue decomposition of an $N \times N$ matrix, where the constant hidden in the big-O notation is actually quite large, especially when the layer involves absorptive medium.

As in [20], we calculate the DtN map for each layer based on the Chebyshev collocation method. Without loss of generality, we consider the first layer given by $y_0 < y < y_1$ and discretize y by

$$\xi_k = y_0 + \frac{y_1 - y_0}{2}\left[1 - \cos\left(\frac{k\pi}{q}\right)\right], \quad 0 \le k \le q. \tag{27}$$

Notice that $\xi_0 = y_0$ and $\xi_q = y_1$. The Chebyshev collocation method approximates the derivative through a differentiation matrix C. Let v be a smooth function y and v' be its derivative, then

$$\begin{bmatrix} v'(\xi_0) \\ v'(\xi_1) \\ \vdots \\ v'(\xi_q) \end{bmatrix} \approx C \begin{bmatrix} v(\xi_0) \\ v(\xi_1) \\ \vdots \\ v(\xi_q) \end{bmatrix}.$$

An explicit formula for C is given in Appendix I. Similarly, the second derivative at these discrete points can be approximated by multiplying C^2.

The DtN map $\mathcal{M}^{(1)}$ is related to the boundary value problem: given $u = u_0(x)$ at $y = y_0$ and $u = u_1(x)$ at $y = y_1$, find $\partial_y u$ at y_0^+ and y_1^-, where u satisfies Eq. (4) and the quasi-periodic condition (10). In Appendix I, we show that this boundary value problem is related to $q-1$ ordinary differential equations:

$$\rho_1 \frac{d}{dx}\left(\frac{1}{\rho_1}\frac{dw_k}{dx}\right) + (k_0^2\varepsilon_1 + \mu_k)w_k = -\delta_k u_0(x) - \zeta_k u_1(x), \tag{28}$$

for $1 \le k < q$, where $\varepsilon_1 = \varepsilon_1(x)$ is the dielectric function of the layer, $\rho_1 = 1$ or ε_1 for the E or H polarization, respectively, μ_k, δ_k and ζ_k are constants related to the matrix C and given in Appendix I. Furthermore, w_k satisfies the same quasi-periodic condition as u, i.e.,

$$w_k(L) = \gamma w_k(0), \quad \left.\frac{1}{\rho_1}\frac{dw_k}{dx}\right|_{x=L^+} = \gamma \left.\frac{1}{\rho_1}\frac{dw_k}{dx}\right|_{x=0^+}. \tag{29}$$

Notice that the equations for w_k are not coupled and they can be solved in parallel. If we solve the boundary value problem (28) and (29) for each k, then $\partial_y u$ at y_0^+ and y_1^- can be evaluated by

$$\partial_y u_0^+ = c_{00}\, u_0 + \sum_{k=1}^{q-1} \eta_k\, w_k + c_{0q}\, u_1, \tag{30}$$

$$\partial_y u_1^- = c_{q0}\, u_0 + \sum_{k=1}^{q-1} \tau_k\, w_k + c_{qq}\, u_1, \tag{31}$$

where c_{00}, c_{0q}, c_{q0} and c_{qq} are the four corner entries of C, η_k and τ_k are also related to C. The details are given in Appendix I. In Section 5, we develop a compact fourth order finite difference scheme for solving w_k, and it requires $O(N)$ operations if x for $0 < x \le L$ is discretized by N points. To find $\partial_y u$ at y_0^+ and y_1^-, we have to find w_k for $1 \le k < q$ and evaluate them by (30) and (31), therefore, the total required number of operations is $O(qN)$.

To calculate $\mathcal{M}^{(1)}$, we have to repeat the boundary value problem N times. From Eq. (15), it is clear that if we choose u_0 as a column of the $N \times N$ identity matrix and u_1 as the zero vector, $\partial_y u_0^+$ and $\partial_y u_1^-$ are corresponding columns of $\mathcal{M}_{11}^{(1)}$ and $\mathcal{M}_{21}^{(1)}$. Therefore, these two matrices can be obtained if we solve N boundary value problems with u_0 going through all columns of the identity matrix. The other two matrices $\mathcal{M}_{12}^{(1)}$ and $\mathcal{M}_{22}^{(1)}$ are obtained from the reflection symmetry. The total required number of operations is thus $O(qN^2)$. Due to the exponential convergence of the Chebyshev collocation method, q is typically much smaller than N. In comparison, Fourier and finite difference modal methods require $O(N^3)$ operations to calculate the eigenvalue decomposition of an $N \times N$ matrix. Of course, the integer N in the Fourier modal method represents the number of terms retained in the

Fourier series, and it could be different from the number of points used to discretize x. In Section 6, we show that our method based on a fourth order finite difference scheme is more accurate than the Fourier modal method when the same N is used.

5. Fourth order finite difference scheme

In a y-invariant layer, the Helmholtz equation is reduced to

$$\rho\frac{\partial}{\partial x}\left(\frac{1}{\rho}\frac{\partial u}{\partial x}\right)+\frac{\partial^2 u}{\partial y^2}+k_0^2\varepsilon\, u=0, \tag{32}$$

where $\varepsilon=\varepsilon(x)$, and $\rho=1$ or $\rho=\varepsilon(x)$ for the E or H polarization, respectively. To simplify the notations, we choose to avoid a specific layer, such as the j-th layer given by $y_{j-1}<y<y_j$ where a subscript j must be attached to ε and ρ. We discretize one period of x by

$$x_l=lh \quad \text{for} \quad 0\le l\le N, \tag{33}$$

where $h=L/N$ is the grid size. If $\phi(x)$ is a function of x with continuous sixth order derivative, we have the following well-known three-point fourth order finite difference formula:

$$\frac{1}{h^2}\left[\phi(x_{l-1})-2\phi(x_l)+\phi(x_{l+1})\right]=\frac{1}{12}\left[\phi''(x_{l-1})+10\phi''(x_l)+\phi''(x_{l+1})\right]+O(h^4). \tag{34}$$

In [24], Chiou *et al* generalized (34) to the x-derivative term in (32) under the assumption that $\varepsilon(x)$ is piecewise constant. In the following, we present the method with some simplification.

Since $\varepsilon(x)$ is piecewise constant, it is possible that $\varepsilon(x)$ is discontinuous at some grid points. Therefore, we consider x-derivatives of u at the right limit of the grid points. To further simplify the notations, we let $\phi_l=u(x_l^+,y)$, $\phi_l'=\partial_x u(x_l^+,y)$, $\phi_l''=\partial_x^2 u(x_l^+,y)$, ..., and define the following column vector

$$\Phi_l=\left[\,\phi_l \quad \phi_l' \quad \phi_l'' \quad \phi_l''' \quad \phi_l^{(4)} \quad \phi_l^{(5)}\,\right]^T.$$

As in [24] and also given in the Appendix II, there are two 6×6 matrices F and G satisfying

$$\Phi_{l-1}\approx F\,\Phi_l, \quad \Phi_{l+1}\approx G\,\Phi_l. \tag{35}$$

These two matrices are related to k_0, ε and the locations of the discontinuities (if any) between x_{l-1}^+ and x_{l+1}^+, and they are derived from Taylor expansions and the boundary conditions at the discontinuities. Assuming that the entries of F and G are f_{ij} and g_{ij} for $0\le i,j\le 5$, we can re-write the first and third rows of (35) as

$$\begin{bmatrix}\phi_{l-1}-f_{00}\,\phi_l-f_{02}\,\phi_l''\\ \phi_{l+1}-g_{00}\,\phi_l-g_{02}\,\phi_l''\\ \phi_{l-1}''-f_{20}\,\phi_l-f_{22}\,\phi_l''\\ \phi_{l+1}''-g_{20}\,\phi_l-g_{22}\,\phi_l''\end{bmatrix}\approx\begin{bmatrix}f_{01}&f_{03}&f_{04}\\ g_{01}&g_{03}&g_{04}\\ f_{21}&f_{23}&f_{24}\\ g_{21}&g_{23}&g_{24}\end{bmatrix}\begin{bmatrix}\phi_l'\\ \phi_l'''\\ \phi_l^{(4)}\end{bmatrix}, \tag{36}$$

where the terms associated with $\phi_l^{(5)}$ are ignored. Clearly, there is a row vector of length 4 such that its product with the 4×3 matrix at the right hand side of (36) is a zero vector. We denote the row vector by $[a_l, c_l, -d_l, -f_l]$, then its product with the left hand side of (36) gives

$$[\, a_l \quad b_l \quad c_l \,] \begin{bmatrix} \phi_{l-1} \\ \phi_l \\ \phi_{l+1} \end{bmatrix} - [\, d_l \quad e_l \quad f_l \,] \begin{bmatrix} \phi''_{l-1} \\ \phi''_l \\ \phi''_{l+1} \end{bmatrix} \approx 0, \tag{37}$$

where

$$[\, b_l \quad e_l \,] = [\, -a_l \quad -c_l \quad d_l \quad f_l \,] \begin{bmatrix} f_{00} & f_{02} \\ g_{00} & g_{02} \\ f_{20} & f_{22} \\ g_{20} & g_{22} \end{bmatrix}. \tag{38}$$

We can re-scale the coefficients such that $d_l + e_l + f_l = 1$, then (37) is the generalization of (34). The truncation error is related to $\phi_l^{(5)}$ and it is $O(h^3)$ in general. However, if the discontinuities of ε are located at the grid points or the midpoints between two nearby grid points, then formula (37) has an $O(h^4)$ error. The six coefficients $\{a_l, b_l, ..., f_l\}$ can be easily calculated numerically, once the matrices F and G are formed. Chiou *et al* derived these coefficients using additional approximations [24].

Using the finite difference formula (37), we can easily semi-discretize Eq. (32) as

$$A_2^{-1} A_1 \vec{\phi} + \partial_y^2 \vec{\phi} + k_0^2 A_0 \vec{\phi} = 0, \tag{39}$$

where $\vec{\phi} = [\phi_1, \phi_2, ..., \phi_N]^T$, $A_0 = \text{diag}\{\varepsilon(x_1^+), \varepsilon(x_2^+), ..., \varepsilon(x_N^+)\}$ is the diagonal matrix for $\varepsilon(x)$, A_1 and A_2 are periodic tridiagonal matrices given as

$$A_1 = \begin{bmatrix} b_1 & c_1 & & & a_1/\gamma \\ a_2 & b_2 & c_2 & & \\ & a_3 & b_3 & \ddots & \\ & & \ddots & \ddots & c_{N-1} \\ \gamma c_N & & & a_N & b_N \end{bmatrix}, \quad A_2 = \begin{bmatrix} e_1 & f_1 & & & d_1/\gamma \\ d_2 & e_2 & f_2 & & \\ & d_3 & e_3 & \ddots & \\ & & \ddots & \ddots & f_{N-1} \\ \gamma f_N & & & d_N & e_N \end{bmatrix}.$$

To obtain (39), we re-write the Helmholtz equation (32) at x_l^+ as

$$\phi''_l + \partial_y^2 \phi_l + k_0^2 \varepsilon(x_l^+)\, \phi_l = 0,$$

and use the quasi-periodic condition in the following form:

$$\phi_0 = \frac{1}{\gamma} \phi_N, \quad \phi_{N+1} = \gamma \phi_1.$$

Now we consider Eq. (28) for w_k. Since w_k is a linear combination of $u(x, \xi_l)$ for $1 \le l < q$, it satisfies the same boundary conditions at material discontinuities, and can be discretized by the same finite difference scheme. Therefore, Eq. (28) is approximated by

$$\left(A_2^{-1} A_1 + \mu_k I + k_0^2 A_0 \right) \vec{w}_k = \vec{p}_k, \tag{40}$$

where A_0, A_1 and A_2 are associated with $\varepsilon_1(x)$, and $\vec{p}_k$ is the column vector whose l-th element is $-\delta_k u_0(x_l) - \zeta_k u_1(x_l)$. We can re-write Eq. (40) as

$$\left(A_1 + \mu_k A_2 + k_0^2 A_2 A_0\right) \vec{w}_k = A_2 \vec{p}_k. \tag{41}$$

Since the coefficient matrix of the above system is periodic tridiagonal, it can be solved using $O(N)$ operations. To calculate the DtN map $\mathcal{M}^{(1)}$, we have to repeat the boundary value problem N times for each fixed k. This corresponds to different right hand sides of the linear system (41). We can save computation time by calculating the LU decomposition of the coefficient matrix in (41) only once.

6. Numerical examples

In this section, we present some numerical examples to illustrate the performance of our method. The first example is a metallic lamellar grating as shown in Fig. 2. The refractive

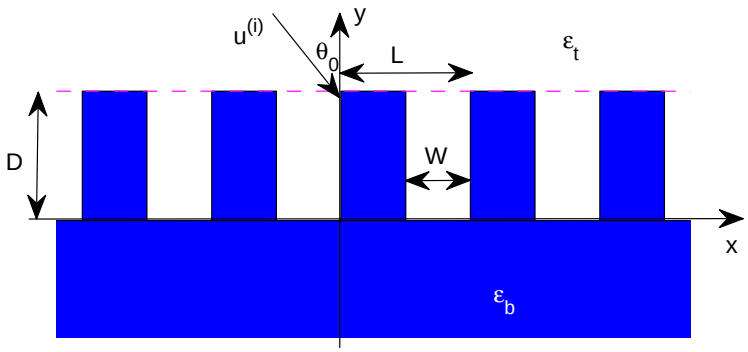

Fig. 2. A metallic lamellar grating.

index of the metal is $n = 0.22 + 6.71i$. The medium above the metal is air. The interface has a simple rectangular shape and it is periodic in the x direction with period L. The height and the width of the grooves are $D = L$ and $W = L/2$, respectively. We consider a plane incident wave with a free space wavelength $\lambda = 2\pi/k_0 = L$ and an angle of incidence $\theta_0 = 30°$. This example has been previously analyzed by a number of authors [8, 9, 11, 12].

First, we test the accuracy of the fourth order finite difference scheme presented in Section 5 by calculating the fundamental mode of the uniform layer ($0 < y < D$). In such a layer, the Helmholtz equation (4) has modal solutions given as $u = \phi(x)e^{i\beta y}$, where ϕ satisfies the differential equation

$$\rho \frac{d}{dx}\left(\frac{1}{\rho}\frac{d\phi}{dx}\right) + k_0^2 \varepsilon\, \phi = \beta^2 \phi, \quad 0 < x < L \tag{42}$$

and the quasi-periodic condition (10). In the layer, the dielectric function ε is a function of x only, and $\rho = 1$ or $\rho = \varepsilon$ for the E or H polarization, respectively. The finite difference scheme in Section 5 gives rise to the matrix eigenvalue problem

$$\left(A_1 + k_0^2 A_2 A_0\right) \vec{\phi} = \beta^2 A_2 \vec{\phi}, \tag{43}$$

where A_0, A_1 and A_2 are given in Section 5 and β^2 is the eigenvalue. The fundamental mode corresponds to a β with the largest real part. For this simple example, the exact β can be solved analytically [4]. We have $\beta L = 2.548836809 + 0.03587408322i$ and $\beta L = 6.601779613 + 0.01131390971i$ for the E and H polarizations, respectively. Based on these accurate values, we can calculate the relative error $\mathrm{err}(\beta) = |(\beta - \beta^{(N)})/\beta|$, where $\beta^{(N)}$ is the numerical solution obtained using N points to discretize one period of x. For comparison, we also calculate the fundamental mode by a Fourier series expansion method as in the Fourier modal method [10]. In that case, N denotes the number of terms retained in the Fourier series. The results are shown in Fig. 3 for both polarizations. The fourth order accuracy of

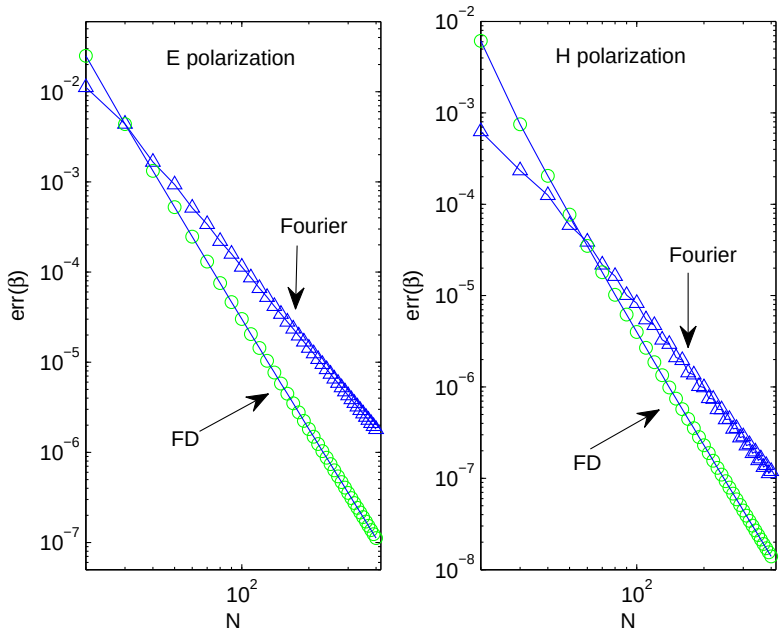

Fig. 3. Relative errors $\mathrm{err}(\beta)$ of the fundamental mode for Example 1, calculated by the finite difference and Fourier series expansion methods.

the finite difference method can be easily observed, as the error lines (in logarithmic scale) have the slope -4. Notice that the Fourier series expansion method performs quite well for small N, but the finite different method is more accurate when N is large.

For this example, only the minus-first and zeroth reflected orders are propagating. In Tables 1 and 2, we show calculated diffraction efficiencies of the zeroth reflected order for the E and

Table 1. Diffraction efficiencies of the zeroth reflected order for various truncation orders N (E polarization).

N	FMM	DtN(q=20)	DtN(q=25)	DtN(q=30)
20	0.76233	0.78126	0.78125	0.78125
30	0.74569	0.74441	0.74440	0.74440
50	0.73675	0.73554	0.73553	0.73553
70	0.73518	0.73460	0.73459	0.73459
90	0.73470	0.73440	0.73439	0.73439
120	0.73445	0.73432	0.73431	0.73431
160	0.73435	0.73430	0.73429	0.73429
200	0.73432	0.73429	0.73428	0.73428

Table 2. Diffraction efficiencies of the zeroth reflected order for various truncation orders N (H polarization).

N	FMM	DtN(q=20)	DtN(q=25)	DtN(q=30)
20	0.83128	0.84623	0.84624	0.84624
30	0.83986	0.84765	0.84766	0.84766
50	0.84527	0.84854	0.84855	0.84855
70	0.84636	0.84859	0.84858	0.84858
90	0.84688	0.84858	0.84857	0.84857
120	0.84759	0.84857	0.84855	0.84855
160	0.84779	0.84856	0.84854	0.84853
200	0.84794	0.84855	0.84854	0.84852

H polarizations, respectively. The reflected diffraction efficiency of the j-th order is defined as $\mathrm{RE}_j = \mathrm{Re}[|R_j|^2 \beta_j^{(t)}/\beta_0^{(t)}]$. In particular, $\mathrm{RE}_0 = |R_0|^2$. For comparison, solutions obtained by FMM are also listed in the two tables. These results are shown for various values of N and q, where N is defined before and q is the number of points for discretizing y. Based on an adaptive spatial resolution technique, Granet previously obtained some accurate results for this problem [11]. Up to the first five significant digits, the exact values are $\mathrm{RE}_0 = 0.73428$ and $\mathrm{RE}_0 = 0.84848$ for the E and H polarizations, respectively. From Table 1 for the E polarization, it is clear that our method gives all 5 correct digits for $N = 200$ and $q = 25$ or

30, but FMM produces only 4 correct digits for the same N. For the H polarization, we have obtained all correct 5 digits using $N = 400$ and $q = 30$. As listed in Table 2, for $N = 200$ and $q = 30$, our method gives $\mathrm{RE}_0 = 0.84852$ and FMM gives $\mathrm{RE}_0 = 0.84794$. The corresponding absolute errors are 0.00004 and 0.00054, respectively. To reveal more details, we calculate the relative errors of the reflection coefficients defined as $\mathrm{err}(R_j) = |(R_j^{(N)} - R_j)/R_j|$, where R_j denotes an accurate reference value and $R_j^{(N)}$ denotes the numerical solution associated with N discretization points or N Fourier terms. In Fig. 4, we show the relative errors of

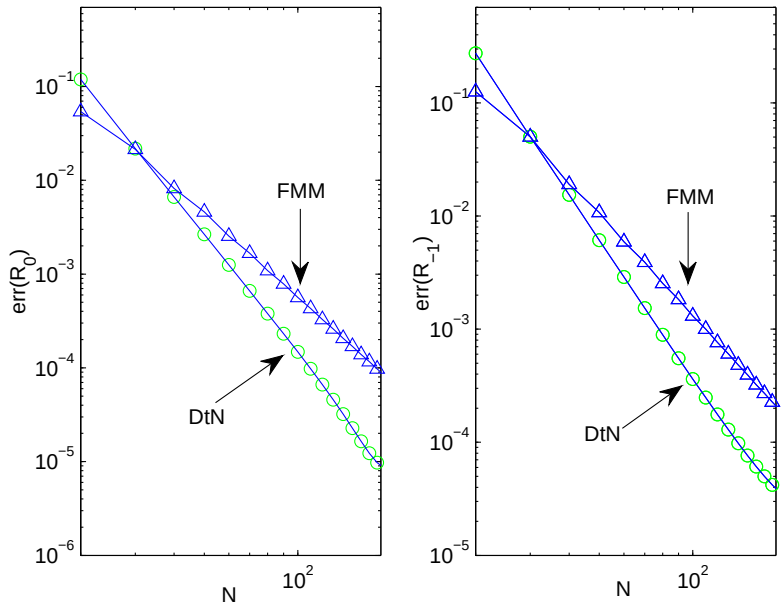

Fig. 4. Relative errors of the reflection coefficients R_0 (left) and R_{-1} (right) for the E polarization, calculated using the Fourier modal method and the DtN map method.

R_0 and R_{-1} for the E polarization and compare our method with FMM. It is clear that our method is more accurate than FMM when N is moderately large.

For this example, we also compare the computation time of our method and FMM. On a Intel PC with a 2.4GHz CPU, based on our implementation in MATLAB, we observe that the two methods require about the same time (0.5 s) for $N = 100$, but for larger N our method is clearly more efficient. For $N = 200$ and $N = 400$, our method requires 1.7 s and 6.9 s, respectively, which are roughly 40% of the computation time required by FMM.

For the second example, we consider a dielectric grating with a stair-step profile as shown in Fig. 5. The dielectric medium has a refractive index $n = 1.58$. The interface follows a

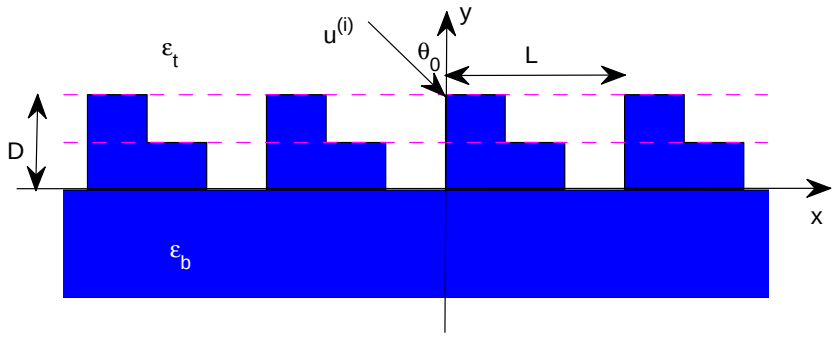

Fig. 5. Grating with a stair-step profile.

simple stair-step profile with the horizontal distance of $L/3$ and the vertical distance of $D/2$ per step, where L is the period in x and D is the depth of the groove. The medium above the interface is air. We consider a plane incident wave with an angle of incidence $\theta_0 = 30°$. As in [26], we first analyze the structure for various values of D/L at the fixed free space wavelength $\lambda = L$. In Fig. 6, we show the diffraction efficiencies of the three transmitted orders for the E polarization. In that case, the diffraction efficiency of the j-th transmitted order is defined as $\mathrm{TE}_j^{(e)} = \mathrm{Re}\,[|T_j|^2\beta_j^{(b)}/\beta_0^{(t)}]$, where $\beta_j^{(b)}$ is given in (9). These results are obtained with $N = 90$ and $q = 30$, and they agree well with those reported in [26]. Next, we fix groove depth at $D = L$ and consider power reflectance and transmittance as functions of the normalized frequency, where the reflectance and transmittance are defined as the sum of all reflected efficiencies and transmitted efficiencies, respectively. The results are shown in Fig. 7. We also calculate the total power (relative to the incident power) as the sum of the transmittance and reflectance and it is indeed very close to one. For the results shown in Fig. 7, the total power only deviates from 1 by a small amount around 10^{-9}.

7. Conclusions

In this paper, we developed a new method for diffraction gratings that are periodic in one direction and layered in the other direction. For each layer, we calculate the Dirichlet-to-Neumann (DtN) map based on a fourth order finite difference scheme for discretizing the periodic direction and a Chebyshev collocation method for discretizing the uniform direction. The DtN map can be calculated using $O(qN^2)$ operations, where N is the number of points used to discretize one period and q is much smaller. Compared with the widely used Fourier modal method (FMM), our method is more efficient since it avoids the eigenvalue decomposition that requires $O(N^3)$ operations. Our method is also more accurate than FMM, if the

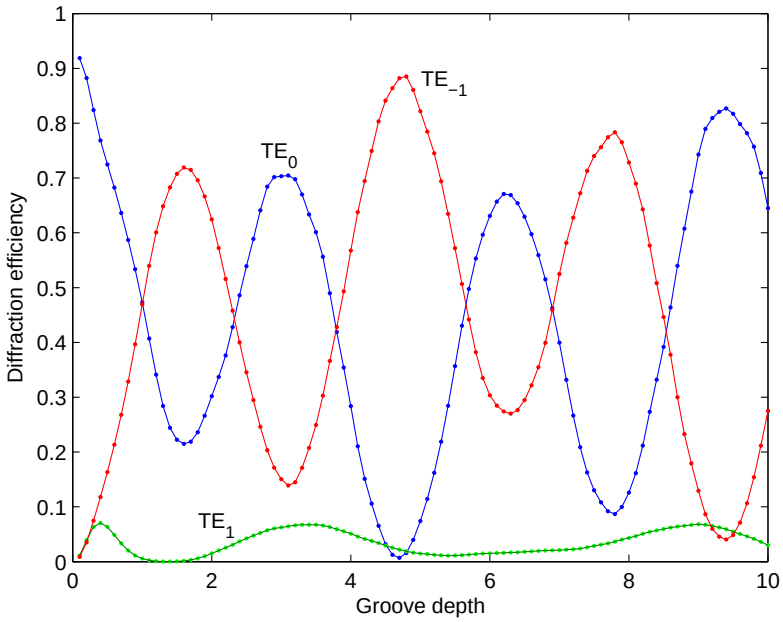

Fig. 6. Diffraction efficiencies of the three transmitted orders as functions of D/L, where D is the groove depth D and L is the period, for a dielectric grating with a stair-step profile.

same N is used for the number of retained terms in Fourier series and when N is not too small.

The accuracy of FMM has been improved by the adaptive spatial resolution (coordinate stretching) technique [11]. We expect that our method can also be improved by using non-uniform mesh in the finite difference scheme. On the other hand, if the structure has many layers with discontinuities at many different locations, adaptive spatial resolution or non-uniform meshing can be quite inconvenient. Our method is suitable for diffraction gratings with uniform layers. For a general grating with sloping interfaces, the usual approach is to approximate it by a multilayered grating. However, it is well-known that the involved staircase approximation may produce large errors for the H polarization [27].

Appendix I

In the first layer $y_0 < y < y_1$, the Helmholtz equation can be written as

$$\partial_y^2 u + \mathcal{L}u = 0, \quad \mathcal{L} = \rho_1 \frac{\partial}{\partial x}\left(\frac{1}{\rho_1}\frac{\partial}{\partial x}\right) + k_0^2 \varepsilon_1.$$

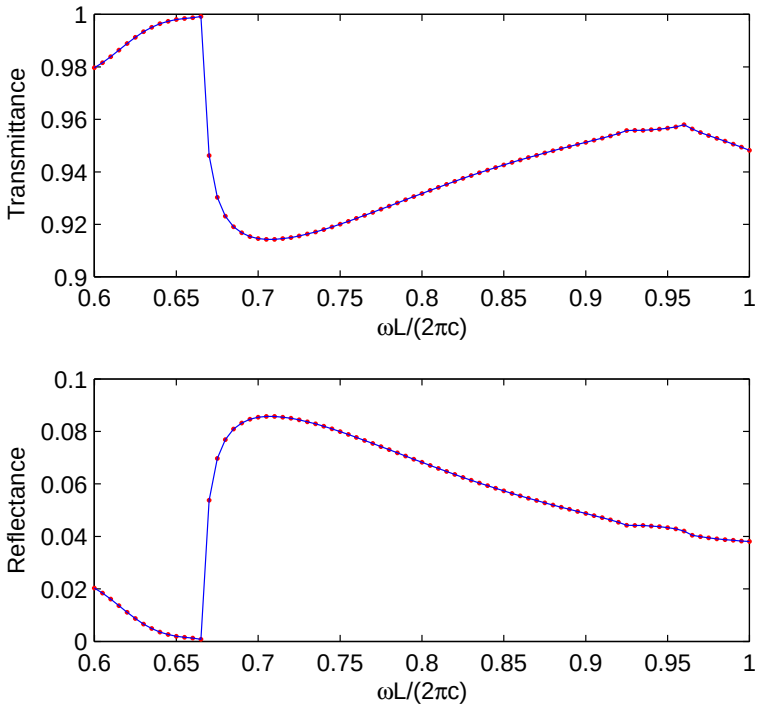

Fig. 7. Power transmittance and reflectance as functions of the normalized frequency for a dielectric grating with a stair-step profile.

For the discretization (27), the entries of C are

$$c_{kl} = -\frac{2}{y_1 - y_0} \begin{cases} (2q^2+1)/6 & \text{if} \quad k = l = 0, \\ -(2q^2+1)/6 & \text{if} \quad k = l = q, \\ -0.5\gamma_k/(1-\gamma_k^2) & \text{if} \quad 0 < k = l < q, \\ (-1)^{k+l}\sigma_k\sigma_l^{-1}/(\gamma_k - \gamma_l) & \text{otherwise,} \end{cases}$$

where $\gamma_k = \cos(k\pi/q)$, $\sigma_0 = \sigma_q = 2$ and $\sigma_k = 1$ for $0 < k < q$. Let us write down the matrices C and C^2 as follows:

$$C = \begin{bmatrix} c_{00} & \tilde{c}_0 & c_{0q} \\ \vdots & \vdots & \vdots \\ c_{q0} & \tilde{c}_q & c_{qq} \end{bmatrix}, \quad C^2 = \begin{bmatrix} d_{00} & \cdots & d_{0q} \\ \hat{d}_0 & \hat{D} & \hat{d}_q \\ d_{q0} & \cdots & d_{qq} \end{bmatrix},$$

where $\tilde{c}_0$ and $\tilde{c}_q$ are row vectors of length $q-1$, $\hat{d}_0$ and $\hat{d}_q$ are column vectors of length $q-1$, and $\hat{D}$ is a $(q-1) \times (q-1)$ matrix.

We assume that the discretized Helmholtz equation is strictly valid at ξ_k for $1 \le k < q$, if

∂_y^2 is approximated by C^2. Therefore

$$\hat{d}_0\, u_0 + \hat{D}U + \hat{d}_q\, u_1 + \mathcal{L}U = 0, \tag{44}$$

where $U = [u(x,\xi_1),\, u(x,\xi_2),\, \cdots,\, u(x,\xi_{q-1})]^T$. We can diagonalize the matrix $\hat{D}$ as

$$\hat{D} = R \begin{bmatrix} \mu_1 & & & \\ & \mu_2 & & \\ & & \ddots & \\ & & & \mu_{q-1} \end{bmatrix} R^{-1},$$

where R is an invertible $(q-1)\times(q-1)$ matrix. We define column vectors $\vec{\delta}$ and $\vec{\zeta}$, and row vectors $\vec{\eta}$ and $\vec{\tau}$ by

$$\vec{\delta} = R^{-1}\hat{d}_0, \quad \vec{\zeta} = R^{-1}\hat{d}_q, \quad \vec{\eta} = \tilde{c}_0 R, \quad \vec{\tau} = \tilde{c}_q R,$$

then Eq. (44) is reduced to (28), where $\vec{w} = R^{-1}U$. If we evaluate $\partial_y u$ at y_0 and y_1 based on the first and last rows of the matrix C, we obtain (30) and (31).

Appendix II

For Helmholtz equation (32) where ε and ρ depend only on x, we consider two grid points x_1 and x_2, and assume that ε is discontinuous at $x_* = x_1 + ah$, where $h = x_2 - x_1$ and $0 < a \le 1$. For u and its x-derivatives, if we use Taylor expansions from x_2^+ to x_*^+ and from x_*^- to x_1^+, we obtain

$$\Phi(x_2^+) \approx T(1-a)\Phi(x_*^+), \quad \Phi(x_*^-) \approx T(a)\Phi(x_1^+),$$

where

$$\Phi(x) = \begin{bmatrix} u(x,z) \\ \partial_x u(x,z) \\ \vdots \\ \partial_x^5 u(x,z) \end{bmatrix}, \quad T(\xi) = \begin{bmatrix} t_0(\xi) & t_1(\xi) & \cdots & t_5(\xi) \\ & t_0(\xi) & \ddots & \vdots \\ & & \ddots & t_1(\xi) \\ & & & t_0(\xi) \end{bmatrix}$$

and $t_j(\xi) = (\xi h)^j/j!$ for $j = 0,\, 1,\, 2,\, ...,\, 5$. Let us assume that

$$\varepsilon(x) = \begin{cases} \varepsilon_1, & x_1 < x < x_* \\ \varepsilon_2, & x_* < x \le x_2, \end{cases}$$

where ε_1 and ε_2 are constants, then the interface conditions give us

$$\Phi(x_*^+) = J\Phi(x_*^-),$$

where

$$J = \begin{bmatrix} 1 & & & & & \\ 0 & \theta & & & & \\ \eta & 0 & 1 & & & \\ 0 & \eta\theta & 0 & \theta & & \\ \eta^2 & 0 & 2\eta & 0 & 1 & \\ 0 & \eta^2\theta & 0 & 2\eta\theta & 0 & \theta \end{bmatrix}, \quad J^{-1} = \begin{bmatrix} 1 & & & & & \\ 0 & 1/\theta & & & & \\ -\eta & 0 & 1 & & & \\ 0 & -\eta/\theta & 0 & 1/\theta & & \\ \eta^2 & 0 & -2\eta & 0 & 1 & \\ 0 & \eta^2/\theta & 0 & -2\eta/\theta & 0 & 1/\theta \end{bmatrix},$$

for $\eta = k_0^2(\varepsilon_1 - \varepsilon_2)$ and $\theta = \rho_2/\rho_1$. Therefore, $\Phi(x_2^+) \approx G\Phi(x_1^+)$ and $\Phi(x_1^+) \approx F\Phi(x_2^+)$ for

$$F = T(-a)\, J^{-1}\, T(a-1), \quad G = T(1-a)\, J\, T(a).$$

Acknowledgments

This research was partially supported by a grant from the Research Grants Council of Hong Kong Special Administrative Region, China (Project No. CityU 102008).

References

1. R. Petit, ed., Electromagnetic Theory of Gratings (Speinger-Verlag, Berlin, 1980).
2. M. Nevière and E. Popov, Light Propagation in Periodic Media, Marcel Dekker, Inc. 2003.
3. G. Bao, Z. M. Chen, and H. J. Wu, "Adaptive finite-element method for diffraction gratings," J. Opt. Soc. Am. A **22**, 1106-1114 (2005).
4. L. C. Botten, M. S. Craig, R. C. McPhedran, J. L. Adams, and J. R. Andrewartha, "The dielectric lamellar diffraction grating," Optica Acta **28**, 413-428 (1981).
5. L. C. Botten, M. S. Craig, R. C. McPhedran, J. L. Adams, and J. R. Andrewartha, "The finitely conducting lamellar diffraction grating," Optica Acta **28**, 1087-1102 (1981).
6. L. C. Botten, M. S. Craig, and R. C. McPhedran, "Highly conducting lamellar diffraction gratings," Optica Acta **28**, 1103-1106 (1981).
7. M. G. Moharam and T. K. Gaylord, "Rigorous coupled-wave analysis of metallic surface-relief gratings," J. Opt. Soc. Am. A **3**, 1780-1787 (1986).
8. P. Lalanne and G. M. Morris, "Highly improved convergence of the coupled-wave method for TM polarization," J. Opt. Soc. Am. A **13**, 779-784 (1996).
9. G. Granet and B. Guizal, "Efficient implementation of the coupled-wave method for metallic lamellar gratings in TM polarization," J. Opt. Soc. Am. A **13**, 1019-1023 (1996).
10. L. Li, "Use of Fourier series in the analysis of discontinuous periodic structures," J. Opt. Soc. Am. A **13**, 1870-1876 (1996).

11. G. Granet, "Reformulation of the lamellar grating problem through the concept of adaptive spatial resolution," J. Opt. Soc. Am. A **16**, 2510-2516 (1999).
12. P. Lalanne and J. P. Hugonin, "Numerical performance of finite-difference modal methods for the electromagnetic analysis of one-dimensional lamellar gratings," J. Opt. Soc. Am. A **17**, 1033-1042 (2000).
13. E. Popov and M. Nevière, "Grating theory: new equations in Fourier space leading to fast converging results for TM polarization," J. Opt. Soc. Am. A **17**, 1773-1784 (2000).
14. E. Popov and M. Nevière, "Maxwell equations in Fourier space: A fast-converging formulation for diffraction by arbitrary shaped, periodic, anisotropic media," J. Opt. Soc. Am. A **18**, 2886-2894 (2001).
15. A. Pomp, "The integral method for coated gratings – computational cost," J. Mod. Opt. **38**, 109-120 (1991).
16. D. W. Prather, M. S. Mirotznik, and J. N. Mait, "Boundary integral methods applied to the analysis of diffractive optical elements," J. Opt. Soc. Am. A **14**, 34-43 (1997).
17. E. Popov, B. Bozhkov, D. Maystre, and J. Hoose, "Integral method for echelles covered with lossless or absorbing thin dielectric layers," Applied Optics **38**, 47-55 (1999).
18. A. Rathsfeld, G. Schmidt, and B. H. Kleemann, "On a fast integral equation method for diffraction gratings," Communications in Computational Physics **1**, 984-1009 (2006).
19. Y. Huang and Y. Y. Lu, "Scattering from periodic arrays of cylinders by Dirichlet-to-Neumann maps," J. Lightwave Technol. **24**, 3448-3453 (2006).
20. L. Yuan and Y. Y. Lu, "An efficient bidirectional propagation method based on Dirichlet-to-Neumann maps," IEEE Photon. Technol. Lett. **18**, 1967-1969 (2006).
21. Y. Huang and Y. Y. Lu, "Modeling photonic crystals with complex unit cells by Dirichlet-to-Neumann maps," Journal of Computational Mathematics **25**, 337-349 (2007).
22. L. Yuan and Y. Y. Lu, "A recursive doubling Dirichlet-to-Neumann map method for periodic waveguides," J. Lightwave Technol. **25**, 3649-3656 (2007).
23. Y. Wu and Y. Y. Lu, "Dirichlet-to-Neumann map method for analyzing interpenetrating cylinder arrays in a triangular lattice," J. Opt. Soc. Am. B **25**, 1466-1473 (2008).
24. Y. P. Chiou, Y. C. Chiang, and H. C. Chang, "Improved three-point formulas considering the interface conditions in the finite-difference analysis of step-index optical devices," J. Lightwave Technol. **18**, 243-251 (2000).
25. G. Bao, D. C. Dobson, and J. A. Cox, "Mathematical studies in rigorous grating theory," J. Opt. Soc. Am. A **12**, 1029-1042 (1995).
26. N. Chateau and J. P. Hugonin, "Algorithm for the rigorous coupled wave analysis of grating diffraction," J. Opt. Soc. Am. A **11**, 1321-1331 (1994).
27. E. Popov, M. Nevière, B. Gralak, and G. Tayeb, "Staircase approximation validity for arbitrary-shaped gratings," J. Opt. Soc. Am. A **19**, 33-42 (2002).